Improving the Photovoltage of Dithienopyrrole Dye-Sensitized Solar Cells via Attaching the Bulky Bis(octyloxy) biphenyl Moiety to the Conjugated π-Linker

Ning Cai, Jing Zhang, Mingfei Xu, Min Zhang, and Peng Wang**

The judicious design of 3D giant organic dye molecules to enable the formation of a porous photoactive layer on the surface of titania is one of the viable tactics to abate the adverse interfacial charge recombination in dye-sensitized solar cells (DSCs) employing outer-sphere redox couples. Here 2′,6′-bis(octyloxy)-biphenyl substituted dithieno[3,2-*b*:2′,3′-*d*]pyrrole segment is constructed and employed as the π-linker of a high molar absorption coefficient organic push-pull dye. With respect to its congener possessing the hexyl substituted dithieno[3,2-*b*:2′,3′-*d*]pyrrole linker, the new dye can self-assemble on the surface of titania to afford a porous organic coating, which effectively slow down the kinetics of charge recombination of titania electrons with both outer-sphere tris(1,10-phenanthroline)cobalt(III) ions and photooxidized dye molecules, improving the cell photovoltage. In addition, the diminishments of charge recombination via modulating the microstructure of interfacial functional zone can also overcompensate the disadvantageous impact of reduced light-harvesting and evoke an enhanced photocurrent output, bringing forth an efficiency improvement from 7.5% to 9.3% at the 100 mW cm^{-2}, simulated AM1.5 conditions.

1. Introduction

During the past two decades, substantial research passions have been fascinated by dye-sensitized solar cells (DSCs)[1,2] in the light of their grand potential to achieve the solar-to-electricity transformation at a low cost, based upon resource-abundant and less energy-intensive materials as well as simple manufacture technologies. The energy gap and energy offsets of a dye molecule, the light-harvesting component of this nanostructured device, with respect to other materials jointly impact the photocarrier generation. In addition, the free energy of output electrons could be considerably modulated by an organic layer mainly composed of dye molecules, lying between titania nanocrystals and redox shuttles. The cutting-edge DSC dyes are ruthenium polypyridyl and zinc porphyrin complexes, exhibiting ≈12% power conversion efficiencies at the air mass 1.5 conditions.[3,4]

N. Cai, J. Zhang, Dr. M. Xu, Dr. M. Zhang, Prof. P. Wang
State Key Laboratory of Polymer Physics and Chemistry
Changchun Institute of Applied Chemistry
Chinese Academy of Sciences
Changchun, 130022, China
E-mail: min.zhang@ciac.jl.cn; peng.wang@ciac.jl.cn

DOI: 10.1002/adfm.201203348

On the other side, much effort has been devoted to metal-free organic D-π-A dyes, primarily owing to the flexibility of molecular design.[5,6] The elaborate option of conjugated π-linkers is one of the executable tactics towards energy-level engineering of organic D-π-A dyes,[7] apart from electron donors and acceptors. In this respect, a great amount of organic dyes involving thiophene and its numerous derivative segments have been exploited[8–14] since the work by Arakawa et al.[15] on the coumarin-thiophene DSC chromophores. Amongst all metal-free dyes, so far only a few dyes featuring either dithienosilole (DTS) or cyclopentadithiophene (CPDT) have been demonstrated to exhibit over 10% efficiencies.[16–18] However the preparations of DTS and CPDT typically involve cryogenic temperatures and hazardous organolithium reagents.

Thereby the dithieno[3,2-*b*:2′,3′-*d*]pyrrole (DTP) unit pioneered by Rasmussen et al.[19] as a promising building block of electronic materials has been exploited as the electron-donor or π-linker of metal-free organic dyes.[12,20] It is valuable to note that the triphenylamine-cyanoacrylic acid dye with the DTP linker displays a higher molar extinction coefficient than its counterparts with DTS and CPDT, ensuring a comparable photocurrent generation. Unfortunately, an inferior photovoltage was observed for the **C241** dye with the 4-hexyl-4*H*-dithieno[3,2-*b*:2′,3′-*d*]pyrrole linker (**Figure 1**A).[12] Recent studies on DSCs with outer-sphere electron mediators have suggested that the extraordinary merit of devising bulky organic dyes for high open-circuit photovoltage cells.[4,18,21–24] In this work, we will synthesize the 4-(2′,6′-bis(octyloxy)biphenyl-4-yl)-4*H*-dithieno[3,2-*b*:2′,3′-*d*]pyrrole segment and employ it as the π-conjugated linker of a new dye coded **C251** (Figure 1A), and further compare its electrochemical, photophysical, and photovoltaic characteristics with respect to the reference DTP dye **C241**.

2. Results and Discussion

As depicted in **Scheme 1**, **C251** was prepared according to a previously reported procedure of the Suzuki–Miyaura cross-coupling of a pinacol bisarylaminophenyl boronate with

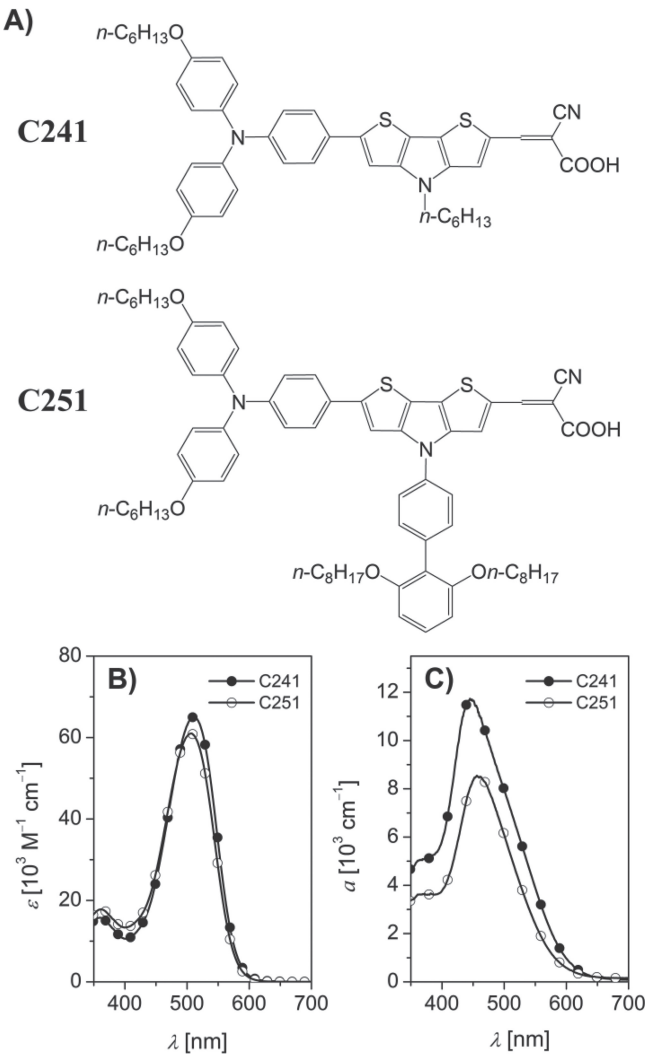

Figure 1. A) Chemical structures of two dithienopyrrole dyes investigated in this work. B) Electronic absorption spectra of the THF dye solutions. C) Absorption spectra of the dye-coated titania films.

a bromine substituted aromatic aldehyde,[12] and the widely deployed Knoevenagel condensation to produce a cyanoacrylic acid DSC dye.[25,26] Bisoctyloxy substituted iodobenzene **2** was almost quantitatively obtained by alkylation of 2-iodobenzene-1,3-bis(olate) in the polar aprotic solvent of acetone. By virtue of a highly active phosphine ligand of 2-(2′,6′-dimethoxybiphenyl) dicyclohexylphosphine (SPhos),[27] the hindered iodide **2** was successfully cross-coupled at a moderate temperature with 4-(4,4,5,5-tetramethyl-1,3,2-dioxaborolan-2-yl)benzenamine in excellent yield to afford amine **3**, which further underwent the Buchwald–Hartwig amination of 3,3′-dibromo-2,2′-bithiophene to give the key intermediate **4** in excellent yield. Aldehyde **5** was obtained in excellent yield by the selective monoformylation of **4** via the Vilsmeier–Haack reaction, and further brominated with *N*-bromosuccinimide (NBS) to generate the key intermediates **6**. Note that the bromination must be carried out at a low temperature of ≈0 °C to avoid the side reaction on the bis(octyloxy) phenyl moiety.

The electronic absorption spectra of diluted THF solutions of **C241** and **C251** were first recorded to evaluate the molecular-level capacity of solar radiation capture. As depicted in Figure 1B, a slightly lower maximum molar absorption coefficient (ε^{abs}_{max}) of 61×10^3 M^{-1} cm^{-1} at 506 nm was measured for the **C251** dye, compared to that of 65×10^3 M^{-1} cm^{-1} at 511 nm for **C241**. The experimentally measured blue-shifting of absorption peak and the decrease of absorption coefficient from **C241** to **C251** can be nicely reproduced by the TDDFT calculations on the maximum absorption wavelength (λ_{max}) and the corresponding oscillator strengths (*f*) listed in Table S1 of the Supporting Information. Less intense and blue-shifted absorption of **C251** in comparison to **C241** is mainly related to the small increase from 18 to 20° of the torsion angle between the phenyl and DTP moieties. Further analyses on the molecular orbital topologies (**Figure 2**) involving the $S_0 \rightarrow S_1$ transitions disclose that the low-energy absorption bands of **C241** and **C251** are mainly assigned to the intramolecular charge transfer transitions from the triphenylamine donor to the cyanoacrylic acid acceptor. It is also worthy of noting that

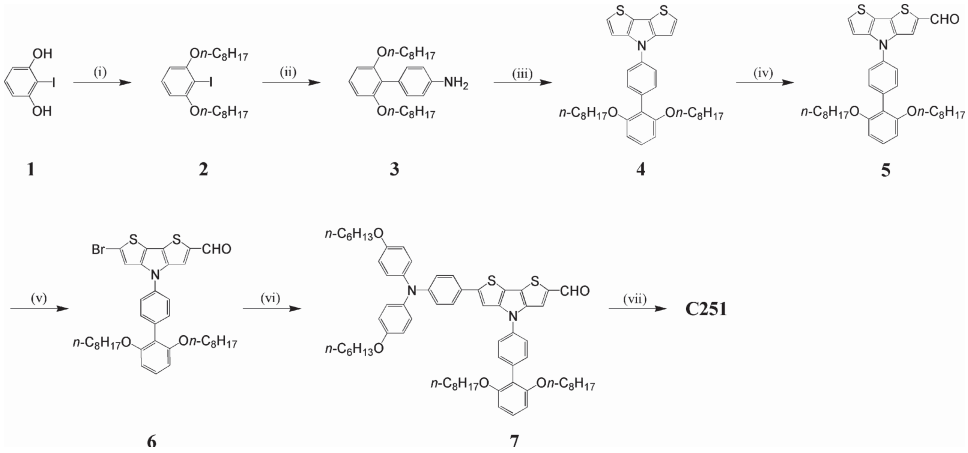

Scheme 1. Synthetic route of the **C251** dye. Reagents and conditions: i) 1-bromooctane, K_2CO_3, acetone, reflux; ii) 4-(4,4,5,5-tetramethyl-1,3,2-dioxaborolan-2-yl)benzenamine, $Pd(OAc)_2$, SPhos, K_3PO_4, dioxane/H_2O (*v*/*v*, 5/1), rt; iii) 3,3′-dibromo-2,2′-bithiophene, $Pd_2(dba)_3$, BINAP, NaO*t*-Bu, toluene, reflux; iv) DMF, $POCl_3$, 1,2-dichloroethane, rt; v) NBS, THF, 0 °C; vi) 4,4,5,5-tetramethyl-2-{4-[*N*,*N*-bis(4-hexyloxyphenyl)amino]phenyl}-1,3,2-dioxaborolane, $Pd(OAc)_2$, SPhos, K_3PO_4, dioxane/H_2O (*v*/*v*, 5/1), rt; vii) cyanoacetic acid, piperidine, $CHCl_3$, reflux.

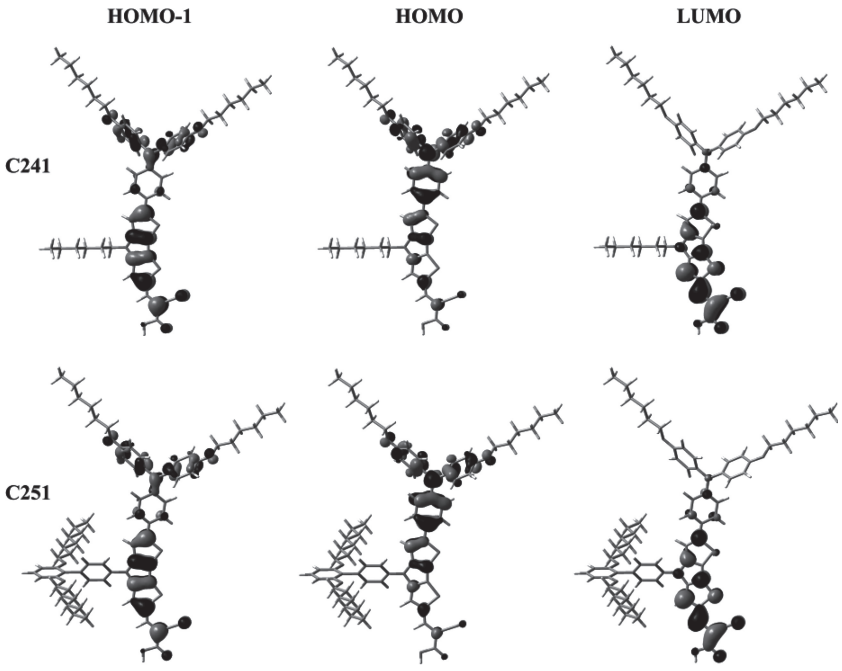

Figure 2. Distribution of frontier molecular orbitals involving the $S_0 \rightarrow S_1$ transitions of **C241** and **C251** in THF. All the iodensity surface values are fixed at 0.03.

there is nearly no distribution of these frontier orbitals on the 2′,6′-bis(octyloxy)-biphenyl moiety, which could be considered as an insulating spacer to reduce the intermolecular exciton annihilation in the assembly of dye molecules grafted on the surface of titania.

The attenuation of intermolecular interaction in the assembly of DTP dye molecules via attaching the 2′,6′-bis(octyloxy)-biphenyl group was further supported by recording the progressive blue-shifting of absorption peaks (Figure S1, Supporting Information) during the dyeing of titania. The shift of absorption peak is less evident for **C251** during the dying process than **C241**, suggesting that **C241** is prone to aggregate on the surface of titania. We also measured the electronic absorption of a stained titania film reaching the stage of adsorption-desorption equilibrium, which is more closely related to the DSC light-harvesting capacity. As presented in Figure 1C, lower absorption coefficients (a) in the whole visible region are noted for a dyed film with **C251** than **C241**. The measured dye load amounts of **C241** and **C251** are 2.8×10^{-8} and 1.4×10^{-8} mol cm^{-2} μm^{-1}, respectively, which could be rationalized in terms of the geometries (Figure S2, Supporting Information) of **C241** and **C251**.

The substituent related intermolecular interaction was further assessed by measuring the cyclic voltammograms of dye-coated titania films at various scan rates, to probe the diffusive lateral charge transfer characteristics[28–30] in the electroactive dye layer on titania. The ground-state redox potentials E_{D/D^+} of **C241** and **C251** grafted on titania can be precisely derived through averaging the anodic and cathodic peak potentials shown in **Figure 3**A, being 0.28 and 0.32 V versus the ferrocene/ferrocenium (Fc/Fc^+) reference, respectively. Furthermore, the peak current of anodic wave (i_{pa}) can be nicely correlated with the scan rate (v) in terms of the following equation of $i_{pa} = (2.69 \times 10^5) A_s c_m n^{3/2} D_{app}^{1/2} v^{1/2}$.[31] At a given film geometry with invariant electrode area (A_s), film thickness, and porosity, the dye concentration (c_m) is proportional to the dye load amount. Herein, n is the transferred electron number and D_{app} refers to the apparent charge diffusion coefficient. Through comparing the fitting slopes of data shown in Figure 3B, the D_{app} in the molecular layer composed of the hexyl substituted DTP dye is ~4 times higher than that of the 2′,6′-bis(octyloxy)-biphenyl substituted DTP counterpart, proving a stronger intermolecular electronic interaction for **C241** with respect to **C251**.

We further carried out the incident photon-to-collected electron conversion efficiency (IPCE) measurement of a dye-coated titania film in conjunction with an acetonitrile (MeCN) electrolyte containing the tris(1,10-phenanthroline)cobalt(II)/(III) redox couple. The cell details are described in the experimental section. As shown in **Figure 4**A, the **C251** cell exhibits a broad plateau with similar IPCE summit compared

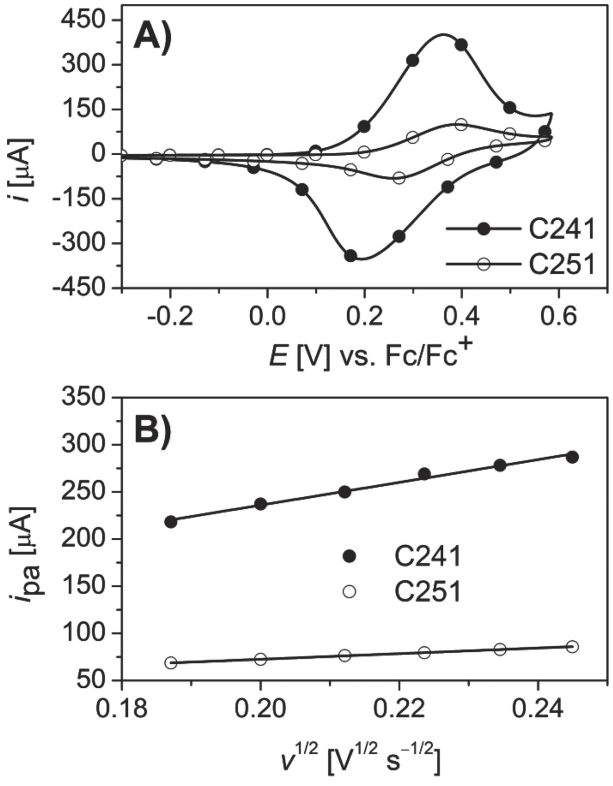

Figure 3. A) Cyclic voltammograms of the dye-coated titania films in 1-ethyl-3-methylimidazolium bis(trifluoromethanesulfonyl)imide. Scan rate: 60 mV s^{-1}. B) Plots of anodic peak current (i_{pa}) as a function of the square root of scan rate ($v^{1/2}$). The solid lines are fitting in terms of equation $i_{pa} = (2.69 \times 10^5) A_s c_m n^{3/2} D_{app}^{1/2} v^{1/2}$.

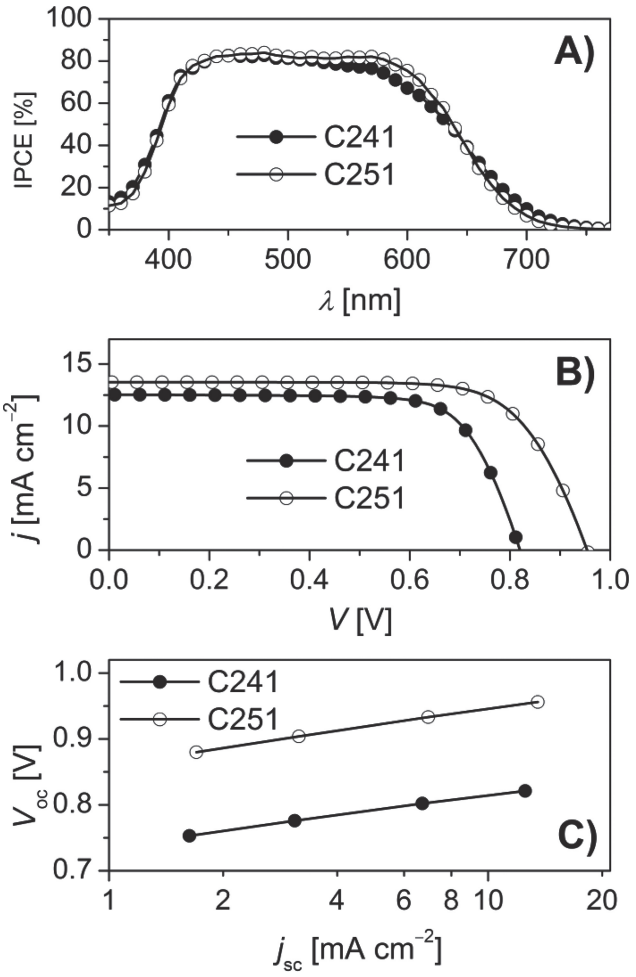

Figure 4. A) Photocurrent action spectra. B) *j–V* characteristics measured at an irradiation of 100 mW cm^{-2} AM1.5 sunlight. C) Plots of open-circuit photovoltage as a function of short-circuit photocurrent density. Cells were tested using a metal mask with an aperture area of 0.158 cm^2. An antireflection film was adhered to the testing cell during measurements.

to the **C241** counterpart. However, it is valuable to notice that the **C241** confers relatively lower IPCEs from 550 to 630 nm, in spite of higher absorptions of the **C241** dye-coated titania film in this spectral region (Figure S3, Supporting Information), suggesting that the **C251** dye can endow a titania film to display an improved charge collection efficiency compared to **C241**.

The solar-to-electricity conversion efficiencies of DSCs made with **C241** and **C251** as the photosensitizers were examined by recording the photocurrent density–voltage (*j–V*) characteristics at the 100 mW cm^{-2}, simulated AM1.5 conditions, and the detailed photovoltaic parameters were compiled in **Table 1**. As Figure 4B presents, the short-circuit photocurrent density (j_{sc}), open-circuit photovoltage (V_{oc}), and fill factor (FF) of the **C241** cell are 12.53 mA cm^{-2}, 0.82 V, and 0.73, respectively, affording a power conversion efficiency (η) of 7.5%. Furthermore, a notably improved V_{oc} of 0.96 V concomitant with an increased j_{sc} of 13.53 mA cm^{-2} was achieved with the **C251** dye, contributing to a higher η of 9.3%. Note that the efficiency of the **N719** dye under the same device condition is only ≈3%. It is known that

Table 1. Photovoltaic parameters obtained at the simulated AM1.5 conditions.[a)]

dye	calculated j_{sc} [mA cm^{-2}]	j_{sc} [mA cm^{-2}]	V_{oc} [V]	FF	η [%]
C241	12.33	12.53	0.82	0.73	7.5
C251	13.40	13.53	0.96	0.72	9.3

[a)] The validity of our photovoltaic data is confirmed by comparing the calculated j_{sc} via wavelength integration of the product of the standard AM1.5 emission spectrum (ASTM G173-03) and measured IPCE spectrum with the experimental j_{sc}, showing a less than 5% error. Also note that all our cells show a linear dependence of photocurrent on light intensity as shown in Figure S4, Supporting Information.

the j_{sc} of DSCs is measured at the condition of a considerable low electron density in the mesoporous titania film, which can significantly reduce the charge recombination flux, thereby it is roughly proportional to the photocarrier generation flux. This estimation has motivated us to compare the dye structure correlated V_{oc} variation at a certain j_{sc} by measuring *j–V* curves under various metal-mesh attenuated lights and plotting V_{oc} as a function of j_{sc}, as presented in Figure 4C. It is noted that at a given j_{sc}, the **C251** cell exhibits an obviously higher V_{oc} than **C241**.

For an invariable redox electrolyte in DSCs, the rise or fall of V_{oc} originates from an upward or downward displacement of electron quasi-Fermi-level ($E_{F,n}$) in titania, which intrinsically stems from a change of titania conduction band edge (E_c) and/or a fluctuation of electron density.[32–35] At a given photocarrier generation flux, the electron density is determined by the interfacial recombination rate of titania electrons with electron accepting species in electrolytes and/or dye cations. We further performed charge extraction and transient photovoltage decay measurements to scrutinize the origins of V_{oc} variation. As depicted in **Figure 5**A, two type of cells made with **C241** and **C251** display a similar extracted electron density (d_n) at the same potential bias, indicative of a fixed conduction-band edge of titania with respect to the electrolyte Fermi-level. As Figure 5B presents, an over one order of magnitude longer charge recombination lifetime (τ_n) for the **C251** cell is however measured compared to the **C241** congener at a given d_n, accounting for the aforementioned superior photovoltage at a given j_{sc}.

Obviously, albeit an evident reduction of dye load amount, the replacement of the linear hexyl group with the bulky 2′,6′-bis(octyloxy)-biphenyl moiety must endow dye molecules to form a more favorite organic layer to inhibit the charge recombination, at the interface between the redox shuttle and titania. To further picture the microstructure of the dye molecule layers, we first measured their damping effect on the escape of photoelectrons from titania to vacuum. Note that in some previous work[18,36,37] the intensity (I) of Ti2p$_{3/2}$ signal in X-ray photoelectron spectroscopy (XPS) measurements has been correlated to the charge recombination at the titania/electrolyte interface. Herein evident reductions of both Ti2p$_{3/2}$ and Ti2p$_{1/2}$ signal intensities (**Figure 6**) can also be perceived for the **C241** or **C251** dye-coated titania film in comparison with the bare substrate.

If the dye coating on titania is compact and vertically homogeneous, the Ti2p$_{3/2}$ intensity from a dye-coated titania film can be quantitatively described with a two-layer model

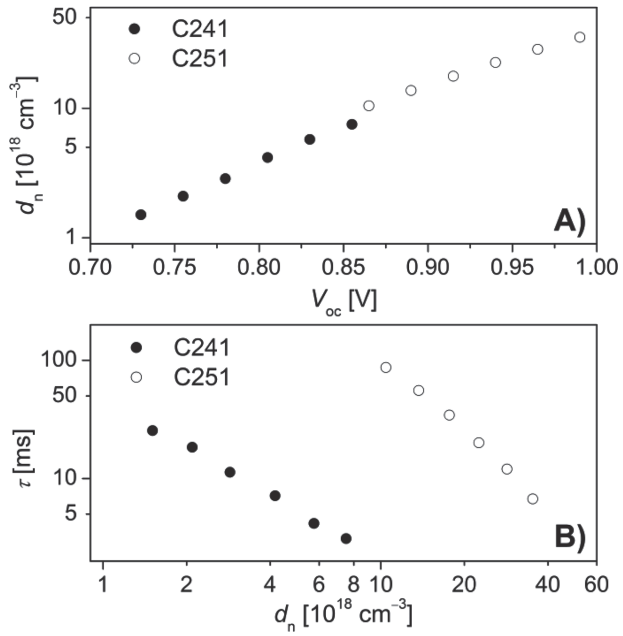

Figure 5. Plots of A) extracted electron density in titania against open-circuit photovoltage and B) electron lifetime as a function of extracted electron density.

$I = I_0\exp(-d/\lambda\sin\alpha)$,[38] where I_0 is the intensity of a titania substrate without dye coating, α is the electron take-off angle of 90°, λ is the inelastic mean free path (IMFP) of electrons in a compact organic solid composed of dye molecules, and d is the mean thickness of a compressed dye layer. The λ values of **C241** and **C251** calculated by means of semi-empirical equations and parameters[39] are 31.3 and 31.2 Å, respectively. On the basis of $Ti2p_{3/2}$ intensities compiled in Table S2, Supporting Information, the compressed mean thicknesses of dye coatings on titania are calculated to be 25.9 and 21.2 Å for **C241** and **C251**. Note that there is not a positive correlation between the thickness estimated by XPS and the electron lifetime evaluated by transient photovoltage decay. This scenario suggests that

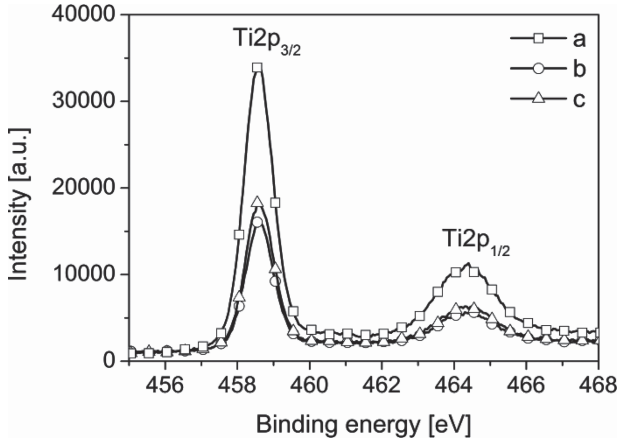

Figure 6. $Ti2p_{3/2}$ and $Ti2p_{1/2}$ photoelectron signals of titania films uncoated (a) and coated by (b) **C241** and (c) **C251**.

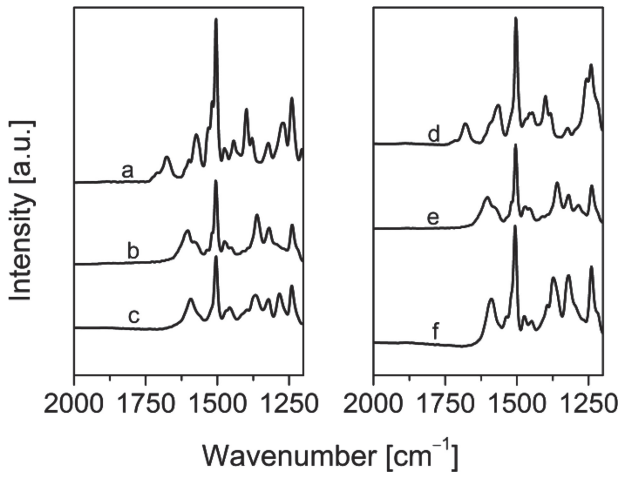

Figure 7. ATR-FTIR spectra of **C241** (a), **C241**Na (b), **C251** (d), and **C251**Na (e) spin-coated on flat quartz as well as **C241** (c) and **C251** (f) grafted on mesoporous titania.

with respect to **C241**, the three-dimensional giant **C251** dye molecules should form a larger porosity organic coating on the surface of titania, however the diameter of resultant micropores should be still smaller than that of tris(1,10-phenanthroline) cobalt(III) ions. This finding has highlighted the necessity of constructing an efficient porous dye layer on the surface of titania through judicious molecular engineering to restrain the adverse interfacial charge recombination with outer-sphere redox shuttles.[35]

The chemical bonding behaviors[40,41] of **C241** and **C251** on titania were further investigated with the aid of attenuated total reflection Fourier transform infrared (ATR-FTIR) spectrum measurements. In contrast to dye films spin-coated on a flat quartz showing the characteristic absorption bands of carboxylic acid (1677 cm^{-1} for **C241**; 1679 cm^{-1} for **C251**, **Figure 7**), both the corresponding deprotonated sodium salt forms on quartz and dye-coated titania films present two new absorption bands (1603 and 1361 cm^{-1} for **C241**Na; 1602 and 1360 cm^{-1} for **C251**Na; 1592 and 1367 cm^{-1} for **C241**/titania; 1589 and 1372 cm^{-1} for **C251**/titania), which can be assigned to the asymmetric and symmetric stretching of carboxylate group.[42] The carboxylic acid absorption bands are not observed for two dye-coated titania films, which can rule out the possibility of dye multilayer formation however still can not confirm a monolayer.

The relative mean tilt angles of dye molecules with respect to the titania surface were analyzed by measuring the charge recombination kinetics of photoinjected electrons in titania and oxidized dye molecules. The validity of this analysis was based on the similar electronic backbone of these two photosensitizers as well as the comparable distribution of titania surface states in our cells. In our experiments, we selected the probe light of 765 nm in joint consideration of strong absorptions in the near-infrared region of these oxidized dye molecules[12] and the signal sensitivity of our photomultiplier tube detector. To ensure a similar charge carrier distribution profile in the testing samples, the excitation wavelengths were carefully chosen according to an optical density of ~0.2 for the

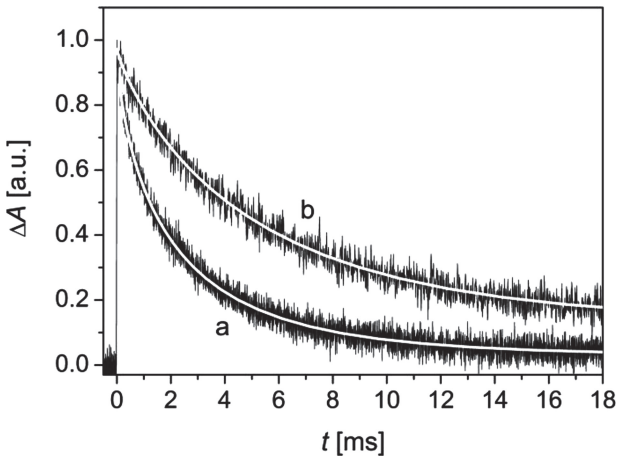

Figure 8. Absorption decay traces recorded at 765 nm of 13-μm-thick, **C241** (a) and **C251** (b) coated titania films in contact with an inert electrolyte upon pulsed laser excitation. Laser pulse fluence: 11 μJ cm^{-2}; excitation wavelength: 663 nm (**C241**) and 652 nm (**C251**). Smooth lines are stretched exponential fittings over raw data obtained by averaging 500 laser shots.

dye-coated titania films infiltrated with an inert electrolyte consisting of 0.5 M 4-*tert*-butylpyridine (TBP) and 0.1 M lithium bis(trifluoromethanesulfonyl)imide (LiTFSI) in MeCN. The absorption traces (**Figure 8**) can be fitted to a stretched exponential decay function $\Delta A \propto A_0 \exp[-(t/\tau)^{\alpha}]$, where A_0 is the pre-exponential factor, α is the stretching parameter, and τ is the characteristic time. By use of the gamma function $\Gamma(x)$, the mean times of these charge recombination reaction ($<\tau>_{rec}$) were derived through $<\tau> = (\tau/\alpha)\Gamma(1/\alpha)$,[43] being 2.7 and 5.7 ms for **C241** and **C251**, respectively. It is obvious that replacing the hexyl unit with 2′,6′-bis(octyloxy)-biphenyl brings forth an evident deceleration of charge recombination, although the **C251** dye has a 40 meV larger Gibbs free energy for this electron transfer reaction, which is estimated based on the aforementioned E_{D/D^+} in Figure 3. By correlating the reduced electron transfer rate to a longer tunneling distance between titania electrons and triphenylamine holes,[44,45] we image that with respect to **C241** there is a smaller tilt angle of the **C251** dye molecules anchored on the surface of titania probably due to its 3D steric encumbrance, as pictorially illustrated in **Scheme 2**, which comes up based upon the preceding theoretical and experimental information.

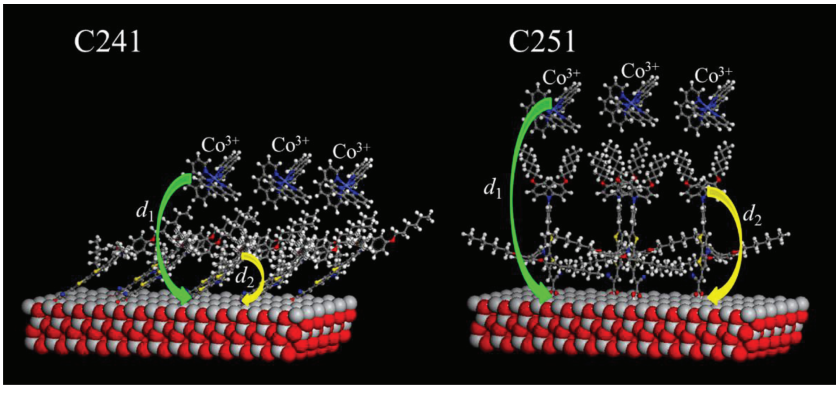

Scheme 2. Pictorial adsorptions of **C241** and **C251** on the surface of titania proposed on the basis of joint experimental and theoretical data. The tunneling distances of two charge transfer channels of photoinjected electrons in titania with the tris(1,10-phenanthroline)cobalt(III) ions (d_1) and dye cations (d_2) are both longer for **C251** than **C241**.

3. Conclusions

To summarize, we have synthesized a new push-pull dye featuring the 4-(2′,6′-bis(octyloxy)biphenyl-4-yl)-4*H*-dithieno[3,2-*b*:2′,3′-*d*]pyrrole π-linker, which presents a power conversion efficiency 9.3% at the 100 mW cm^{-2}, simulated AM1.5 conditions. The attachment of this insulating three-dimensional branched moiety to the conjugated electronic backbone of dye molecules brings forth enhanced photocurrent and photovoltage in comparison with the linear hexyl group. Transient absorption and photovoltage decay measurements have disclosed that the new dye can form a powerful porous photoactive layer on the surface of TiO_2 nanocrystals to decelerate the charge recombination kinetics involving photoinjected titania electrons. The strategy presented here on the construction of a three-dimensional dithienopyrrole dye could be extended to the design of other infrared absorption DSC dyes for more efficient cells employing the single-electron redox shuttles or solid hole-transporters, on account that the significant control of charge recombination in these devices is a big challenge.

4. Experimental Section

Materials: MeCN, *tert*-butanol (*t*-BuOH), phosphorus oxychloride ($POCl_3$), and DMF were distilled before use. $Pd(OAc)_2$, SPhos, NBS, tris(dibenzylideneacetone)dipalladium ($Pd_2(dba)_3$), and (±)-2,2′-bis(diphenylphosphino)-1,1′-binaphthalene (BINAP) were purchased from Sigma-Aldrich and used without any purification. **C241**,[12] 4,4,5,5-tetramethyl-2-{4-[*N*,*N*-bis(4-hexyloxyphenyl)amino]phenyl}-1,3,2-dioxaborolane,[46] 2-iodobenzene-1,3-diol (**1**),[47] 4-(4,4,5,5-tetramethyl-1,3,2-dioxaborolan-2-yl)benzenamine,[48] and 3,3′-dibromo-2,2′-bithiophene[49] were synthesized according to the corresponding literature methods. The synthetic details of **C251** are described as follows.

2-Iodo-1,3-bis(octyloxy)benzene (**2**): To a stirred solution of **1** (10.000 g, 42.371 mmol) and K_2CO_3 (29.280 g, 211.855 mmol) in acetone (200 mL) was added 1-bromooctane (32.730 g, 169.484 mmol). The mixture was refluxed under argon overnight and then cooled to room temperature before filtering and washing with dichloromethane. After evaporation of the filtrate under reduced pressure, the crude product was purified by column chromatography over silica gel with petroleum ether as eluent to obtain a colorless oil as the desired product **2** (18.729 g, 96% yield). ^{1}H NMR (600 MHz, DMSO-d_6, δ): 7.24 (t, J = 8.4 Hz, 1H), 6.58 (d, J = 8.4 Hz, 2H), 4.00 (t, J = 6.3 Hz, 4H), 1.71 (m, 4H), 1.47 (m, 4H), 1.26 (m, 16H), 0.86 (t, J = 6.9 Hz, 6H). ^{13}C NMR (150 MHz, DMSO-d_6, δ): 158.42, 129.93, 105.26, 78.67, 68.62, 31.16, 28.62, 28.56, 25.52, 22.03, 13.91. MS (ESI) m/z calcd. for $C_{22}H_{37}IO_2$: 460.2. Found: 461.1 ($[M+H]^+$). Anal. calcd. for $C_{22}H_{37}IO_2$: C, 57.39; H, 8.10. Found: C, 57.31; H, 8.14.

4-Amino-2′,6′-bis(octyloxy)-biphenyl (**3**): To a stirred solution of **2** (2.000 g, 4.343 mmol),

4-(4,4,5,5-tetramethyl-1,3,2-dioxaborolan-2-yl)benzenamine (0.793 g, 3.620 mmol), and K_3PO_4 (3.842 g, 18.100 mmol) in dioxane/H_2O (106 mL, *v*/*v*, 5/1) was added $Pd(OAc)_2$ (0.016 g, 0.072 mmol) and SPhos (0.030 g, 0.072 mmol). The resulting mixture was stirred at 45 °C under argon for 24 h and then cooled to room temperature. The solution was extracted with ethyl acetate before the organic phase was washed with water and dried over anhydrous sodium sulfate. After evaporation of the solvent under reduced pressure, the crude product was purified by column chromatography over silica gel with dichloromethane/petroleum ether (*v*/*v*, 2/1) as eluent to obtain a colorless oil as the desired product **3** (1.418 g, 92% yield). ^{1}H NMR (600 MHz, DMSO-d_6, δ): 7.12 (t, J = 8.4 Hz, 1H), 6.91 (d, J = 8.4 Hz, 2H), 6.63 (d, J = 8.4 Hz, 2H), 6.51 (d, J = 8.4 Hz, 2H), 4.94 (s, 2H), 3.83 (t, J = 6.3 Hz, 4H), 1.52 (m, 4H), 1.27 (m, 8H), 1.22 (m, 12H), 0.86 (t, J = 7.2 Hz, 6H). ^{13}C NMR (150 MHz, DMSO-d_6, δ): 156.69, 146.79, 131.34, 127.50, 120.91, 120.00, 112.70, 105.56, 67.73, 31.14, 28.63, 28.47, 25.35, 22.04, 13.92. MS (ESI) *m*/*z* calcd. for ($C_{28}H_{43}NO_2$): 425.3. Found: 426.4 ([M+H]$^+$). Anal. calcd. for $C_{28}H_{43}NO_2$: C, 79.01; H, 10.18; N, 3.29. Found: C, 79.11; H, 10.24; N, 3.17.

4-(2′,6′-Bis(octyloxy)biphenyl-4-yl)-4H-dithieno[3,2-b:2′,3′-d]pyrrole (**4**): To a solution of 3,3′-dibromo-2,2′-bithiophene (0.326 g, 1.006 mmol) in toluene (9 mL) was added NaO*t*-Bu (0.230 g, 2.414 mmol), $Pd_2(dba)_3$ (0.022 g, 0.025 mmol), and BINAP (0.062 g, 0.101 mmol) under argon. The resulting mixture was stirred for 30 min before **3** (0.430 g, 1.011 mmol) was added. The reaction was refluxed for 20 h and then cooled to room temperature. Water (10 mL) was added to quench the reaction and the solution was extracted with ethyl acetate before the organic phase was washed with water and dried over anhydrous sodium sulfate. After evaporation of the solvent under reduced pressure, the crude product was purified by column chromatography over silica gel with dichloromethane/petroleum ether (*v*/*v*, 1/2) as eluent to obtain a colorless oil as the desired product **4** (0.561 g, 95% yield). ^{1}H NMR (600 MHz, DMSO-d_6, δ): 7.63 (d, J = 8.4 Hz, 2H), 7.47 (d, J = 4.8 Hz, 2H), 7.46 (d, J = 8.4 Hz, 2H), 7.30 (d, J = 5.4 Hz, 2H), 7.27 (t, J = 8.4 Hz, 1H), 6.74 (d, J = 8.4 Hz, 2H), 3.92 (t, J = 6.6 Hz, 4H), 1.56 (m, 4H), 1.25 (m, 4H), 1.13 (m, 16H), 0.72 (t, J = 6.6 Hz, 6H). ^{13}C NMR (150 MHz, DMSO-d_6, δ): 156.59, 143.26, 137.13, 132.48, 131.76, 129.02, 124.58, 120.43, 118.44, 116.22, 112.43, 105.62, 68.05, 31.09, 28.65, 28.56, 25.44, 21.97, 13.74. MS (ESI) *m*/*z* calcd. for ($C_{36}H_{45}NO_2S_2$): 587.3. Found: 588.4 ([M+H]$^+$). Anal. calcd. for $C_{36}H_{45}NO_2S_2$: C, 73.55; H, 7.72; N, 2.38. Found: C, 73.39; H, 7.80; N, 2.29.

4-(2′,6′-Bis(octyloxy)biphenyl-4-yl)-4H-dithieno[3,2-b:2′,3′-d]pyrrole-2-carbaldehyde (**5**): To a solution of **4** (0.470 g, 0.799 mmol) and DMF (0.174 mL, 2.237 mmol) in 1,2-dichloroethane (10 mL) was added $POCl_3$ (0.087 mL, 0.945 mmol). The resulting mixture was stirred at room temperature under argon for 10 h and then saturated sodium acetate aqueous solution (20 mL) was added. After stirred overnight at room temperature, the solution was extracted with dichloromethane before the organic phase was washed with water and dried over anhydrous sodium sulfate. After evaporation of the solvent under reduced pressure, the crude product was purified by column chromatography over silica gel with dichloromethane/petroleum ether (*v*/*v*, 2/1) as eluent to afford a yellow solid as the desired product **5** (0.448 g, 91% yield). ^{1}H NMR (600 MHz, DMSO-d_6, δ): 9.92 (s, 1H), 8.26 (s, 1H), 7.78 (d, J = 5.4 Hz, 1H), 7.69 (d, J = 8.4 Hz, 2H), 7.50 (d, J = 8.4 Hz, 2H), 7.37 (d, J = 5.4 Hz, 1H), 7.28 (t, J = 8.4 Hz, 1H), 6.75 (d, J = 8.4 Hz, 2H), 3.93 (t, J = 6.3 Hz, 4H), 1.56 (m, 4H), 1.24 (m, 4H), 1.10 (m, 16H), 0.69 (t, J = 7.2 Hz, 6H). ^{13}C NMR (150 MHz, DMSO-d_6, δ): 184.16, 156.58, 147.22, 142.51, 140.32, 136.24, 132.58, 130.40, 129.13, 123.71, 122.97, 120.88, 118.38, 116.43, 112.32, 105.68, 68.12, 31.07, 28.62, 28.56, 25.41, 21.94, 13.68. MS (ESI) *m*/*z* calcd. for $C_{37}H_{45}NO_3S_2$: 615.3. Found: 616.2 ([M+H]$^+$). Anal. calcd. for $C_{37}H_{45}NO_3S_2$: C, 72.16; H, 7.36; N, 2.27. Found: C, 72.28; H, 7.45; N, 2.13.

4-(2′,6′-Bis(octyloxy)biphenyl-4-yl)-6-bromo-4H-dithieno[3,2-b:2′,3′-d]pyrrole-2-carbaldehyde (**6**): To a stirred solution of **5** (0.200 g, 0.325 mmol) in THF (15 mL) at 0°C was added NBS (0.058 g, 0.325 mmol). The resulting mixture was stirred at the same temperature under argon for 24 h and then acetone (20 mL) was added to quench the reaction. After evaporation of the solvent under reduced pressure, the crude product was purified by column chromatography over silica gel with dichloromethane/petroleum ether (*v*/*v*, 2/1) as eluent to obtain a yellow solid as the desired product **6** (0.192 g, 85% yield). ^{1}H NMR (400 MHz, DMSO-d_6, δ): 9.92 (s, 1H), 8.23 (s, 1H), 7.68 (d, J = 8.4 Hz, 2H), 7.54 (s, 1H), 7.49 (d, J = 8.4 Hz, 2H), 7.28 (t, J = 8.4 Hz, 1H), 6.75 (d, J = 8.4 Hz, 2H), 3.93 (t, J = 6.0 Hz, 4H), 1.55 (m, 4H), 1.24 (m, 8H), 1.17 (m, 12H), 0.68 (t, J = 6.8 Hz, 6H). ^{13}C NMR (150 MHz, $CDCl_3$, δ): 182.94, 157.13, 145.68, 142.58, 140.88, 136.38, 133.67, 133.00, 129.05, 124.35, 121.57, 120.90, 118.69, 116.64, 115.75, 115.66, 105.34, 68.64, 31.75, 29.26, 29.17, 29.10, 26.00, 22.59, 14.01. MS (ESI) *m*/*z* calcd. for $C_{37}H_{44}BrNO_3S_2$: 693.2. Found: 694.4 ([M+H]$^+$). Anal. calcd. for $C_{37}H_{44}BrNO_3S_2$: C, 63.96; H, 6.38; N, 2.02. Found: C, 64.05; H, 6.47; N, 1.99.

6-{4-[N,N-Bis(4-hexyloxyphenyl)amino]phenyl}-4-(2′,6′-bis(octyloxy)biphenyl-4-yl)-4H-dithieno[3,2-b:2′,3′-d]pyrrole-2-carbaldehyde (**7**): To a stirred solution of **6** (0.146 g, 0.210 mmol), 4,4,5,5-tetramethyl-2-{4-[N,N-bis(4-hexyloxyphenyl)amino]phenyl}-1,3,2-dioxaborolane (0.144 g, 0.252 mmol), and K_3PO_4 (0.233 g, 1.050 mmol) in dioxane/H_2O (6 mL, v/v, 5/1) was added $Pd(OAc)_2$ (1 mg, 0.004 mmol) and SPhos (2 mg, 0.004 mmol). The resulting mixture was stirred overnight at room temperature under argon and then the solution was extracted with ethyl acetate before the organic phase was washed with water and dried over anhydrous sodium sulfate. After evaporation of the solvent under reduced pressure, the crude product was purified by column chromatography over silica gel with ethyl acetate/petroleum ether (v/v, 1/10) as eluent to obtain an orange solid as the desired product **7** (0.220 g, 99% yield). ^{1}H NMR (400 MHz, DMSO-d_6, δ): 9.89 (s, 1H), 8.21 (s, 1H), 7.72 (d, J = 8.4 Hz, 2H), 7.56 (d, J = 8.4 Hz, 2H), 7.56 (s, 1H), 7.49 (d, J = 8.4 Hz, 2H), 7.28 (t, J = 8.4 Hz, 1H), 7.04 (d, J = 8.8 Hz, 4H), 6.91 (d, J = 8.8 Hz, 4H), 6.76 (m, 4H), 3.93 (m, 8H), 1.70 (m, 4H), 1.55 (m, 4H), 1.41 (m, 4H), 1.31 (m, 8H), 1.18, (m, 12H), 1.08 (m, 8H), 0.88 (t, J = 6.8 Hz, 6H), 0.66 (t, J = 6.8 Hz, 6H). ^{13}C NMR (100 MHz, $CDCl_3$, δ): 182.72, 157.15, 155.84, 149.05, 148.76, 148.39, 142.88, 140.08, 139.92, 136.87, 133.13, 132.88, 128.97, 126.90, 126.39, 126.24, 125.44, 121.60, 120.81, 119.88, 118.82, 115.34, 114.81, 106.32, 105.35, 68.64, 68.26, 31.73, 31.59, 29.70, 29.30, 29.24, 29.15, 29.08, 25.97, 25.75, 22.59, 14.01. MS (ESI) *m*/*z* calcd. for $C_{67}H_{82}N_2O_5S_2$: 1058.6. Found: 1059.7 ([M+H]$^+$). Anal. calcd. for $C_{67}H_{82}N_2O_5S_2$: C, 75.95; H, 7.80; N, 2.64. Found: C, 75.87; H, 7.91; N, 2.60.

2-Cyano-3-{6-{4-[N,N-bis(4-hexyloxyphenyl)amino]phenyl}-4-(2′,6′-bis(octyloxy)biphenyl-4-yl)-4H-dithieno[3,2-b:2′,3′-d]pyrrole-2-yl}acrylic acid (**C251**): To a stirred solution of **7** (0.200 g, 0.189 mmol) and cyanoacetic acid (0.048 g, 0.566 mmol) in chloroform (10 mL) was added piperidine (0.130 mL, 1.323 mmol). The resulting mixture was refluxed for 12 h under argon and then cooled to room temperature before acidified with 2 M hydrochloric acid aqueous solution. The solution was extracted with chloroform before the organic phase was washed with water and dried over anhydrous sodium sulfate. After evaporation of the solvent under reduced pressure, the crude product was purified by column chromatography over silica gel with methanol/chloroform (v/v, 1/50) as eluent to afford a purple-black powder as the desired product **C251**. (0.190 g, 89% yield) ^{1}H NMR (400 MHz, DMSO-d_6, δ): 13.38 (s, 1H), 8.51 (s, 1H), 8.22 (s, 1H), 7.70 (d, J = 8.4 Hz, 2H), 7.55 (m, 3H), 7.49 (d, J = 8.4 Hz, 2H), 7.28 (t, J = 8.4 Hz, 1H), 7.04 (d, J = 8.8 Hz, 4H), 6.91 (d, J = 9.2 Hz, 4H), 6.76 (m, 4H), 3.93, (m, 8H), 1.70 (m, 4H), 1.55 (m, 4H), 1.41 (m, 4H), 1.31 (m, 8H), 1.15, (m, 20H), 0.88 (t, J = 6.8 Hz, 6H), 0.66 (t, J = 6.8 Hz, 6H). ^{13}C NMR (100 MHz, $CDCl_3$, δ): 168.99, 157.12, 155.91, 150.51, 150.22, 149.29, 148.54, 143.63, 139.91, 136.54, 133.34, 133.03, 132.76, 128.96, 128.42, 126.97, 126.44, 125.82, 122.03, 121.49, 119.61, 118.69, 116.78, 115.35, 115.01, 106.02, 105.30, 91.98, 68.63, 68.26, 31.73, 31.59, 29.69, 29.30, 29.24, 29.15, 29.06, 25.96, 25.74, 22.58, 14.01. HR-MS (ESI) *m*/*z* calcd. for $C_{70}H_{83}N_3O_6S_2$: 1125.57233. Found: 1124.56597 ([M-H]$^-$). Anal. calcd. for $C_{70}H_{83}N_3O_6S_2$: C, 74.63; H, 7.43; N, 3.73. Found: C, 74.52; H, 7.49; N, 3.66. IR-FTIR (KBr): 1677 cm^{-1} (COOH), 2214 cm^{-1} (CN).

Spectral, Electrochemical, and XPS Measurements: Static electronic absorption and vibration spectra were measured with an Agilent G1103A spectrometer and a BRUKER Vertex 70 FTIR spectrometer, respectively.

Transient absorption decay traces were recorded with a LP920 laser flash photolysis spectrometer using a tunable OPOLett 355II laser to supply the nanosecond excitation pulse. The ground-state redox potentials of dyes grafted on titania were measured on a CHI660C electrochemical workstation in conjunction with a three-electrode electrochemical cell having a platinum gauze, a silver wire, and a dye-coated titania film on FTO. All potentials were reported with Fc/Fc^+ as the internal reference. XPS spectra were recorded with an ESCALAB 250 spectrometer equipped with a hemispherical electron energy analyzer using the Al Kα radiation ($h\nu$ = 1486.6 eV) and an energy step of 0.1 eV. The electron take-off angle was 90°.

Computational Details: The ground state geometries were optimized employing the hybrid B3LYP[50] function and 6-31G** basis set. The solvent effect of THF on geometry has been simulated by the C-PCM method.[51] Frequency analysis was also performed during the structure optimization to ensure that there is no imaginary frequency. Vertical excitation energies were calculated by TDDFT at the MPW1K/6-31G** levels.[52–54] All calculations were carried out with Gaussian 09 program packages.[55]

Cell Fabrication and Characterization: A double layer titania film made via screen-printing on a pre-cleaned fluorine-doped tin oxide (FTO) conducting glass (Nippon Sheet Glass, Solar, 4 mm thick) was deployed as the negative electrode of DSCs presented in this paper. A 4.2-µm-thick translucent layer of 25 nm sized titania particles was first deposited on a FTO glass and further covered with a 5-µm-thick light-scattering layer of 350–450 nm sized titania particles (WER4-O, Dyesol). Preparation procedures of titania nanocrystals, screen-printing pastes, and nanostructured titania films were very similar to those described in a previous paper.[56] A circular titania electrode (≈0.28 cm^2) was dye-loaded by immersing it into a 150 µM dye solution in the mixed solvent of MeCN and *t*-BuOH. The dye-coated titania electrode was assembled with a thermally platinized FTO electrode by use of a 25-µm-thick Surlyn ring to produce a thin-layer electrochemical cell. The infiltrated electrolyte is composed of 0.25 M tris(1,10-phenanthroline)cobalt(II) di[bis(trifluoromethanesulfonyl)imide], 0.05 M tris(1,10-phenanthroline) cobalt(III) tris[bis(trifluoromethanesulfonyl)imide], 0.5 M TBP, and 0.1 M LiTFSI in MeCN. Details on IPCE, *j–V*, charge extraction and photovoltage decay measurements can be found in our previous publication.[37]

Supporting Information

Supporting Information is available from the Wiley Online Library or from the author.

Acknowledgements

N.C. and J.Z. contributed equally to this work. The National Science Foundation of China (No. 91233206, No. 51125015, No. 51203150, and No. 51103146), the National 973 Program (No. 2011CBA00702), the National 863 Program (No. 2011AA050521), and the Key Scientific and Technological Program of Jilin Province (No. 10ZDGG012) are acknowledged for financial support.

Received: November 14, 2012
Revised: December 16, 2012
Published online: February 18, 2013

[1] B. O'Regan, M. Grätzel, *Nature* **1991**, *353*, 737.
[2] B. E. Hardin, H. J. Snaith, M. D. McGehee, *Nat. Photonics* **2012**, *6*, 162.
[3] Q. Yu, Y. Wang, Z. Yi, N. Zu, J. Zhang, M. Zhang, P. Wang, *ACS Nano* **2010**, *4*, 6032.
[4] A. Yella, H.-W. Lee, H. N. Tsao, C. Yi, A. K. Chandiran, M. K. Nazeeruddin, E. W.-G. Diau, C. Y. Yeh, S. M. Zakeeruddin, M. Grätzel, *Science* **2011**, *334*, 629.
[5] A. Mishra, M. K. R. Fischer, P. Bäuerle, *Angew. Chem. Int. Ed.* **2009**, *48*, 2474.
[6] J. N. Clifford, E. Martínez-Ferrero, A. Viterisi, E. Palomares, *Chem. Soc. Rev.* **2011**, *40*, 1635.
[7] Y.-S. Yen, H.-H. Chou, Y.-C. Chen, C.-Y. Hsu, J. T. Lin, *J. Mater. Chem.* **2012**, *22*, 8734.
[8] N. Koumura, Z.-S. Wang, S. Mori, M. Miyashita, E. Suzuki, K. Hara, *J. Am. Chem. Soc.* **2006**, *128*, 14256.
[9] S. Kim, J. K. Lee, S. O. Kang, J. Ko, J.-H. Yum, S. Fantacci, F. De Anglis, D. Di Censo, M. K. Nazeeruddin, M. Grätzel, *J. Am. Chem. Soc.* **2006**, *128*, 16701.
[10] K. R. J. Thomas, Y.-C. Hsu, J. T. Lin, K.-M. Lee, K.-C. Ho, C.-H. Lai, Y.-M. Cheng, P.-T. Chou, *Chem. Mater.* **2008**, *20*, 1830.
[11] Y. Cui, Y. Wu, X. Lu, X. Zhang, G. Zhou, F. B. Miapeh, W. Zhu, Z.-S. Wang, *Chem. Mater.* **2011**, *23*, 4394.
[12] M. Xu, M. Zhang, M. Pastore, R. Li, F. De Angelis, P. Wang, *Chem. Sci.* **2012**, *3*, 976.
[13] Y.-C. Chen, H.-H. Chou, M. C. Tsai, S.-Y. Chen, J. T. Lin, C.-F. Yao, K. Chen, *Chem. Eur. J.* **2012**, *18*, 5430.
[14] S. Haid, M. Marszalek, A. Mishra, M. Wielopolski, J. Teuscher, J.-E. Moser, R. Humphry-Baker, S. M. Zakeeruddin, M. Grätzel, P. Bäuerle, *Adv. Funct. Mater.* **2012**, *22*, 1291.
[15] K. Hara, M. Kurashige, Y. Dan-oh, C. Kasada, A. Shinpo, S. Suga, K. Sayama, H. Arakawa, *New J. Chem.* **2003**, *27*, 783.
[16] W. Zeng, Y. Cao, Y. Bai, Y. Wang, Y. Shi, M. Zhang, F. Wang, C. Pan, P. Wang, *Chem. Mater.* **2010**, *22*, 1915.
[17] H. N. Tsao, J. Burschka, C. Yi, F. Kessler, M. K. Nazeeruddin, M. Grätzel, *Energy Environ. Sci.* **2011**, *4*, 4921.
[18] Y. Cao, N. Cai, Y. Wang, R. Li, Y. Yuan, P. Wang, *Phys. Chem. Chem. Phys.* **2012**, *14*, 8282.
[19] K. Ogawa, S. C. Rasmussen, *J. Org. Chem.* **2003**, *68*, 2921.
[20] D. Sahu, H. Padhy, D. Patra, J.-F. Yin, Y.-C. Hsu, J.-T. Lin, K.-L. Lu, K.-H. Wei, H.-C. Lin, *Tetrahedron* **2011**, *67*, 303.
[21] S. M. Feldt, E. A. Gibson, E. Gabrielsson, L. Sun, G. Boschloo, A. Hagfeldt, *J. Am. Chem. Soc.* **2010**, *132*, 16714.
[22] H. N. Tsao, C. Yi, T. Moehl, J.-H. Yum, S. M. Zakeeruddin, M. K. Nazeeruddin, M. Grätzel, *ChemSusChem* **2011**, *4*, 591.
[23] T. Daeneke, T.-H. Kwon, A. B. Holmes, N. W. Duffy, U. Bach, L. Spiccia, *Nat. Chem.* **2011**, *3*, 211.
[24] X. Zong, M. Liang, C. Fan, K. Tang, G. Li, Z. Sun, S. Xue, *J. Phys. Chem. C* **2012**, *116*, 11241.
[25] K. Hara, K. Sayama, Y. Ohga, A. Shinpo, S. Suga, H. Arakawa, *Chem. Commun.* **2001**, 569.
[26] T. Kitamura, M. Ikeda, K. Shigaki, T. Inoue, N. A. Anderson, X. Ai, T. Lian, S. Yanagida, *Chem. Mater.* **2004**, *16*, 1806.
[27] S. D. Walker, T. E. Barder, J. R. Martinelli, S. L. Buchwald, *Angew. Chem. Int. Ed.* **2004**, *43*, 1871.
[28] T. J. Meyer, G. J. Meyer, B. W. Pfennig, J. R. Schoonover, C. J. Timpson, J. F. Wall, C. Kobusch, X. Chen, B. M. Peek, C. G. Wall, W. Ou, B. W. Erickson, C. A. Bignozzi, *Inorg. Chem.* **1994**, *33*, 3952.
[29] P. Bonhôte, E. Gogniat, S. Tingry, C. Barbé, N. Vlachopoulos, F. Lenzmann, P. Comte, M. Grätzel, *J. Phys. Chem. B* **1998**, *102*, 1498.
[30] G. R. Hutchison, M. A. Ratner, T. J. Marks, *J. Am. Chem. Soc.* **2005**, *127*, 16866.
[31] A. J. Bard, L. R. Faulkner, *Electrochemical Methods: Fundamentals and Applications*, 2nd ed., Wiley, Weinheim **2001**.
[32] B. C. O'Regan, J. R. Durrant, *Acc. Chem. Res.* **2009**, *42*, 1799.
[33] F. Fabregat-Santiago, G. Garcia-Belmonte, I. Mora-Seró, J. Bisquert, *Phys. Chem. Chem. Phys.* **2011**, *13*, 9083.
[34] J. N. Clifford, E. Martínez-Ferrero, E. Polomares, *J. Mater. Chem.* **2012**, *22*, 12415.

[35] T. Stergiopoulos, P. Falaras, *Adv. Energy Mater.* **2012**, *2*, 616.
[36] T. Marinado, M. Hahlin, X. Jiang, M. Quintana, E. M. J. Johansson, E. Gabrielsson, S. Plogmaker, D. P. Hagberg, G. Boschloo, S. M. Zakeeruddin, M. Grätzel, H. Siegbahn, L. Sun, A. Hagfeldt, H. Rensmo, *J. Phys. Chem. C* **2010**, *114*, 11903.
[37] N. Cai, R. Li, Y. Wang, M. Zhang, P. Wang, *Energy Environ. Sci.* **2013**, *6*, 139.
[38] M. F. Hochella, A. H. Carim, *Surf. Sci.* **1988**, *197*, L260.
[39] P. J. Cumpson, *Surf. Interface Anal.* **2001**, *31*, 23.
[40] F. De Angelis, S. Fantacci, A. Selloni, M. Grätzel, M. K. Nazeeruddin, *Nano Lett.* **2007**, *7*, 3189.
[41] M. Pastore, F. De Angelis, *Phys. Chem. Chem. Phys.* **2012**, *14*, 920.
[42] V. Shklover, Y. E. Ovchinnikov, L. S. Braginsky, S. M. Zakeeruddin, M. Grätzel, *Chem. Mater.* **1998**, *10*, 2533.
[43] A. Y. Anderson, P. R. F. Barnes, J. R. Durrant, B. C. O'Regan, *J. Phys. Chem. C* **2011**, *115*, 2439.
[44] H. Imahori, S. Kang, H. Hayashi, M. Haruta, H. Kurata, S. Isoda, S. E. Canton, Y. Infahsaeng, A. Kathiravan, T. Pascher, P. Chábera, A. P. Yartsev, V. Sundström, *J. Phys. Chem. A* **2011**, *115*, 3679.
[45] S. Mathew, H. Iijima, Y. Toude, T. Umeyama, Y. Matano, S. Ito, N. V. Tkachenko, H. Lemmetyinen, H. Imahori, *J. Phys. Chem. C* **2011**, *115*, 14415.
[46] R. Li, J. Liu, N. Cai, M. Zhang, P. Wang, *J. Phys. Chem. B* **2010**, *114*, 4461.
[47] I. Thomsen, K. B. G. Torssell, *Acta Chem. Scand.* **1991**, *45*, 539.
[48] V. Bhalla, R. Tejpal, M. Kumar, R. K. Puri, R. K. Mahajan, *Tetrahedron Lett.* **2009**, *50*, 2649.
[49] G. Lu, H. Usta, C. Risko, L. Wang, A. Facchetti, M. A. Ratner, T. J. Marks, *J. Am. Chem. Soc.* **2008**, *130*, 7670.
[50] A. D. Becke, *J. Chem. Phys.* **1993**, *98*, 1372.
[51] M. Cossi, N. Rega, G. Scalmani, V. Barone, *J. Comput. Chem.* **2003**, *24*, 669.
[52] B. J. Lynch, P. L. Fast, M. Harris, D. G. Truhlar, *J. Phys. Chem. A* **2000**, *104*, 4811.
[53] M. Cossi, V. Barone, *J. Chem. Phys.* **2001**, *115*, 4708.
[54] M. Pastore, E. Mosconi, F. De Angelis, M. Grätzel, *J. Phys. Chem. C* **2010**, *114*, 7205.
[55] M. J. Frisch, G. W. Trucks, H. B. Schlegel, G. E. Scuseria, M. A. Robb, J. R. Cheeseman, G. Scalmani, V. Barone, B. Mennucci, G. A. Petersson, H. Nakatsuji, M. Caricato, X. Li, H. P. Hratchian, A. F. Izmaylov, J. Bloino, G. Zheng, J. L. Sonnenberg, M. Hada, M. Ehara, K. Toyota, R. Fukuda, J. Hasegawa, M. Ishida, T. Nakajima, Y. Honda, O. Kitao, H. Nakai, T. Vreven, J. A. Montgomery, J. E. Peralta, F. Ogliaro, M. Bearpark, J. J. Heyd, E. Brothers, K. N. Kudin, V. N. Staroverov, R. Kobayashi, J. Normand, K. Raghavachari, A. Rendell, J. C. Burant, S. S. Iyengar, J. Tomasi, M. Cossi, N. Rega, N. J. Millam, M. Klene, J. E. Knox, J. B. Cross, V. Bakken, C. Adamo, J. Jaramillo, R. Gomperts, R. E. Stratmann, O. Yazyev, A. J. Austin, R. Cammi, C. Pomelli, J. W. Ochterski, R. L. Martin, K. Morokuma, V. G. Zakrzewski, G. A. Voth, P. Salvador, J. J. Dannenberg, S. Dapprich, A. D. Daniels, Ö. Farkas, J. B. Foresman, J. V. Ortiz, J. Cioslowski, D. J. Fox, Gaussian 09, Revision A.1, Gaussian, Inc., Wallingford, CT **2009**.
[56] P.Wang, S. M. Zakeeruddin, P. Comte, R. Charvet, R. Humphry-Baker, M. Grätzel, *J. Phys. Chem. B* **2003**, *107*, 14336.